Communication

Segregation Characteristics of Pulsed Laser Butt Welding of Hastelloy C-276

GUANGYI MA, DONGJIANG WU, and DONGMING GUO

The microsegregation/macrosegregation of Hastelloy C-276 weld joint in pulsed laser welding was investigated by scanning electron microscopy (SEM), energy-dispersive X-ray spectroscopy (EDS), and electron probe microanalyzer (EMPA). The results indicated that during pulsed laser welding, the microsegregation was weakened compared with other welding process, and then the Brody-Flemings (BF) model with revised k was proposed to evaluate the element microsegregation in solid-solution strengthened Ni-based alloys. Also, no phenomenal macrosegregation was observed in the weld joint compared with the base metal.

DOI: 10.1007/s11661-011-0978-3

Hastelloy C-276 as a Ni-Cr-Mo superalloy with good corrosion resistance is applied widely in the chemical and nuclear energy industries in the recent years. It is important to develop the welding method of Hastelloy C-276. But because of the element segregation during the arc welding, the brittle phases, which significantly impact the mechanical and corrosion properties of Hastelloy C-276, would appear in the weld joint. For an in-depth understanding of the forming mechanisms of the brittle phases during the arc welding, some researchers investigated the segregation characteristic of Hastelloy C-276. Burton *et al.*[1] and Kane[2] carried out the study of surface segregation of Hastelloy C-276 in a high temperature and proposed the basic mechanism of the phase transformation. Their findings provided the basis of the theory for the high-temperature process of Hastelloy C-276. Cieslak *et al.*[3–5] conducted the experimental investigation on the arc welding of Hastelloy C-276 of 3 mm thickness and investigated the effect of segregation resulting from the solidification on the microstructure evolution of nickel-base alloys. The authors concluded that the Hastelloy C series alloys possess weldability; meanwhile, the microstructures, characteristics of crystal phase, and the hot-cracking mechanism involved were analyzed. In 2005, Ahmad *et al.*[6] conducted the electron beam welding of Hastelloy C-276 of 3 mm thickness, obtaining the fine lamellar structure without the detrimental intermetallic compounds in the welding zone. Although electron beam welding provided an optional welding method to achieve the weld joint without the detrimental intermetallic compounds, so far the element segregation of Hastelloy C-276 during the high-energy beam welding process has not been investigated completely, and especially, few studies are available on the laser welding of Hastelloy C-276. Hence, it is necessary to evaluate the influence of laser welding on the element segregation of Hastelloy C-276 to understand comprehensively the phase transformation of Hastelloy C-276 during the welding.

Pulsed laser welding, which is characteristic of the shorter solidification time, has been applied comprehensively in many industrial fields such as the precision welding and dissimilar metal joining to improve the nature of weld joint.[7–9] In the current work, the microsegregation/macrosegregation that is characteristic of weld joint was investigated. According to the analysis of EDS and electron probe microanalyzer (EMPA), it was found that the microsegregation in the weld joint still occurred, and the Brody-Flemings model with revised k was proposed to evaluate the solute distribution during pulsed laser welding. Also, the obvious macrosegregation was not formed.

A pulsed Nd: YAG laser, with the pulse duration of microsecond order, was used to join the Hastelloy C-276 of 0.5 mm thickness, which is the solid-solution-strengthened Ni-base alloy. Table I presents the normal composition of Hastelloy C-276. In the current work, the welding parameters were single-pulse energy 1.5 J, pulse duration 6 ms, frequency 30 Hz, and welding velocity 100 mm/min, respectively. The purity of 99.99 pct argon gas was used as the shielding gas with 0.1 Mpa. After the welding, the welded samples were cut along the vertical direction of weld joint and then grinded and polished sequentially before being etched in the nitromuriatic acid. Then, a Philips XL-30TMP scanning electron microscope (SEM) with the energy dispersive spectrometer (EDS) was used to analyze the grain microstructure and the element distribution at the grain boundary and body. A SHIMADZU EPMA-1600 (Shimadzu Corp., Kyoto, Japan) was employed to analyze the macrosegregation of the elements at the weld joint.

Figure 1 shows the microstructure of the base metal and weld joint. In Figure 1, the solidification subgrain[10] without the visible eutectoid particles was observed in the weld joint, and the grain size in the weld joint was finer than that of the base metal. The finer grain was the result of the nature of rapid cooling in the laser welding, and the solidification of the subgrain indicated that the composition at the solidification subgrain boundary and body were different from that in the base metal.

In the weld joint of Hastelloy C-276, the concerned brittle phases, which are mostly composed of the Ni, Cr, Mo, Fe, and W, are the P and μ phases.[4,10] So the elements Ni, Cr, Mo, Fe, and W were selected as the

GUANGYI MA, Doctorate Candidate, and DONGJIANG WU and DONGMING GUO, Professors, are with the Key Laboratory for Precision and Nontraditional Machining Technology of Ministry of Education, Dalian University of Technology, Dalian, Liaoning Province 116024, P.R. China. Contact e-mail:gyma@mail.dlut.edu.cn
Manuscript submitted July 19, 2011.
Article published online November 9, 2011

primary analysis object in the EDS spectrogram to evaluate the effect of element segregation during the pulsed laser welding.

Figure 2 shows the element composition at the grain boundary and body in the weld joint. A difference of composition at the grain boundary and body was found. Because the brittle phases tend to segregate at the grain boundary, the element composition at the grain boundary is the important reference point to evaluate the transformation of brittle phases. Table II shows the composition at P phase, μ phase, base metal, eutectoid particles in electron beam welding, and grain boundary in pulsed laser welding, respectively. It was observed, as compared with the normal composition of base metal, that the P and μ phases present the obvious enrichment of Mo-W and the significant depletion of Ni. Meanwhile, the segregation of elements at the grain boundary in pulsed laser welding was also found, but the difference of composition from the base metal was less than that in other welding process. The results indicated that, in the pulsed laser welding, the tendency of element segregation was not strong, and the susceptibility to transformation of brittle phase was weakened.

Based on the concept of solidification, the solute distribution of alloying elements in the solid-solution-strengthened Ni-base alloy can be assessed effectively by the Brody-Flemings model[10–13]

$$C_s = kC_0\left[1 - \frac{f_s}{1+\alpha k}\right]^{k-1} \quad [1]$$

where C_s is the solid composition at the solid/liquid interface, C_0 is the nominal alloy composition, f_s is the fraction solid, k is the equilibrium distribution coefficient, and α is a dimensionless parameter.

Because of the rapid solidification during the pulsed laser welding, the compositions of elements at the grain body and boundary were equivalent to that of elements in the beginning and the end of the solidification, respectively. Hence, $k = C_{body}/C_{0.}$[10] Table III shows k

Table I. Normal Composition of Hastelloy C-276 (Weight Percent)

Ni	Cr	Mo	Fe	W	Mn	Si	S	P	C	Co	V
Balanced	14.5 to 16.5	15.0 to 17.0	4.0 to 7.0	3.0 to 4.5	≤1.0	≤0.08	≤0.03	≤0.04	≤0.01	≤2.5	≤0.35

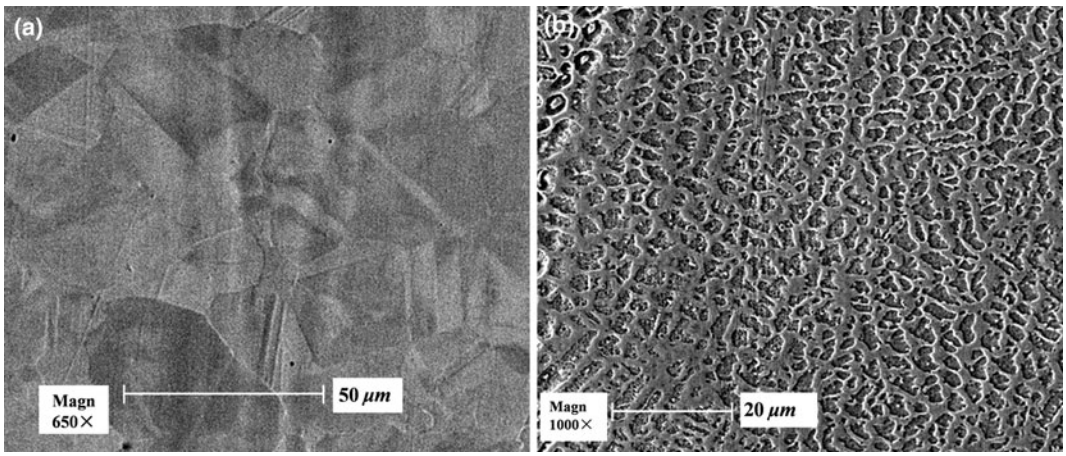

Fig. 1—SEM images: (*a*) base metal microstructure and (*b*) weld joint microstructure.

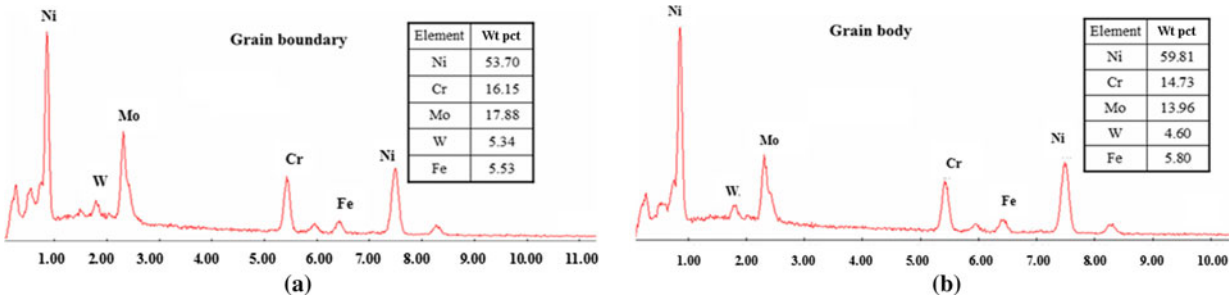

Fig. 2—EDS spectrogram of weld joint: (*a*) grain boundary and (*b*) grain body.

value of different elements in the pulsed laser welding and arc welding. It was interesting to note that the value of k in the pulsed laser welding was not the same as that in the arc welding. Especially in the elements Mo and W, the value of k in the pulsed laser welding was larger than that in the arc welding, which was beneficial to decrease the microsegregation to some extent. That may be because the solute of the larger atom radius (W 2.02 Å and Mo 2.01 Å) compared with the solvent Ni 1.62 Å enhances the difficulty of equilibrium diffusion during the rapid solidification.

In contrast, because of the rapid cooling rate of more than 10^4 °C/s during the pulsed laser welding, the value of α in W, Cr, Mo, and Fe could be set to 0.002, 0.004, 0.0025, and 0.012, respectively.[10,14,15] Putting the value of k and α into the Eq. [1], the solute distribution behavior of Hastelloy C-276 in the pulsed laser welding was obtained as shown in Figure 3(a). The C_s as a function of the fraction solid (f_s) represents the solid composition of solute in the different fraction solid during the solidification. However, the calculated results did not agree with the actual composition at the section of large fraction solid; *i.e.,* when the fraction solid was nearly 1, the calculated composition had an obvious deviation compared with that at the grain boundary. Giovanola and Kurz[16] attributed the deviation calculated by the Brody-Flemings model (BF) to ignore the dendrite tip undercooling and proposed that the Scheil model with the revised k, which stems from the simplification of BF, could be used to evaluate the element distribution at the large fraction solid. Therefore, the value of k should be sectioned according to the different C_s. Based on References 12 and 16, the C_0 was intended to be the sectioned point. When $C_s < C_0$, k is considered as the equilibrium distribution coefficient because of the large fraction liquid. When $C_s \geq C_0$, k would be revised based on the amount of solute enrichment at the grain boundary,[13,16] and the revised value of that, based on the testing results, is shown in Table III. It was found that the revised k approached 1 compared with the k in pulsed laser welding. The result satisfies the fact that the enrichment of solute at the solid/liquid interface, which resulted from the rapid solidification, could increase the concentration of solute

Table II. Composition of Different Phase (Weight Percent)

Crystal Phase	Composition (wt pct)				
	Ni	Mo	Cr	W	Fe
Base metal in heat analysis	58.75	15.7	16.0	3.3	5.6
P[4,10]	34	40	16	7	4
μ[4,10]	33	41	15	6	4
Eutectoid particles in electron beam welding[6]	42.60	29.59	15.50	6.23	4.47
Grain boundary in pulsed laser welding	53.70	17.88	16.15	5.34	5.53

Table III. k Value of Different Solute in Hastelloy C-276

Element	Cr	Mo	W	Fe
In arc welding[10]	0.95	0.82	1.01	1.01
In pulsed laser welding	0.92	0.90	1.39	1.04
Revised undercooling rate > 10^4 °C/s condition	0.98 to 0.99	0.97 to 0.98	0.90 to 0.91	1.00 to 1.01

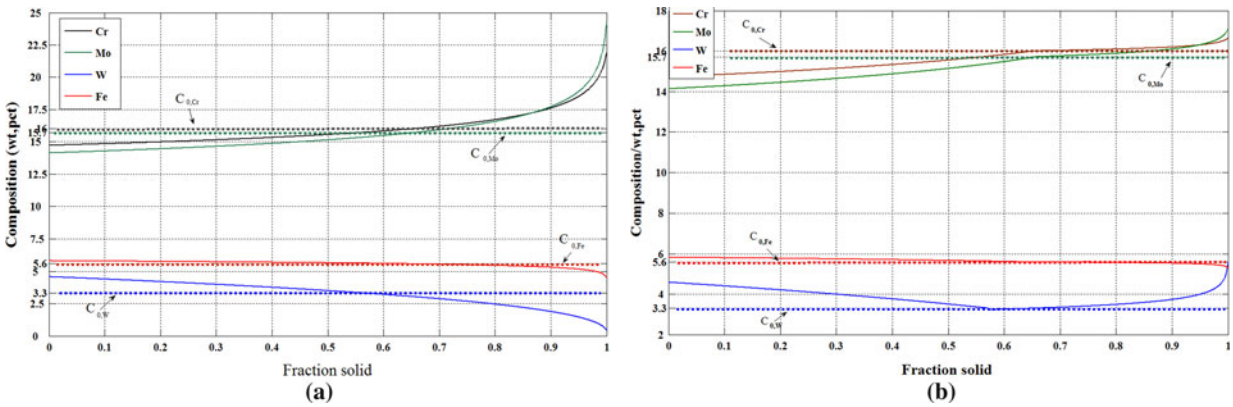

Fig. 3—Solute distribution behavior of Hastelloy C-276 in the pulsed laser welding: (*a*) using BF and (*b*) using BF with revised k.

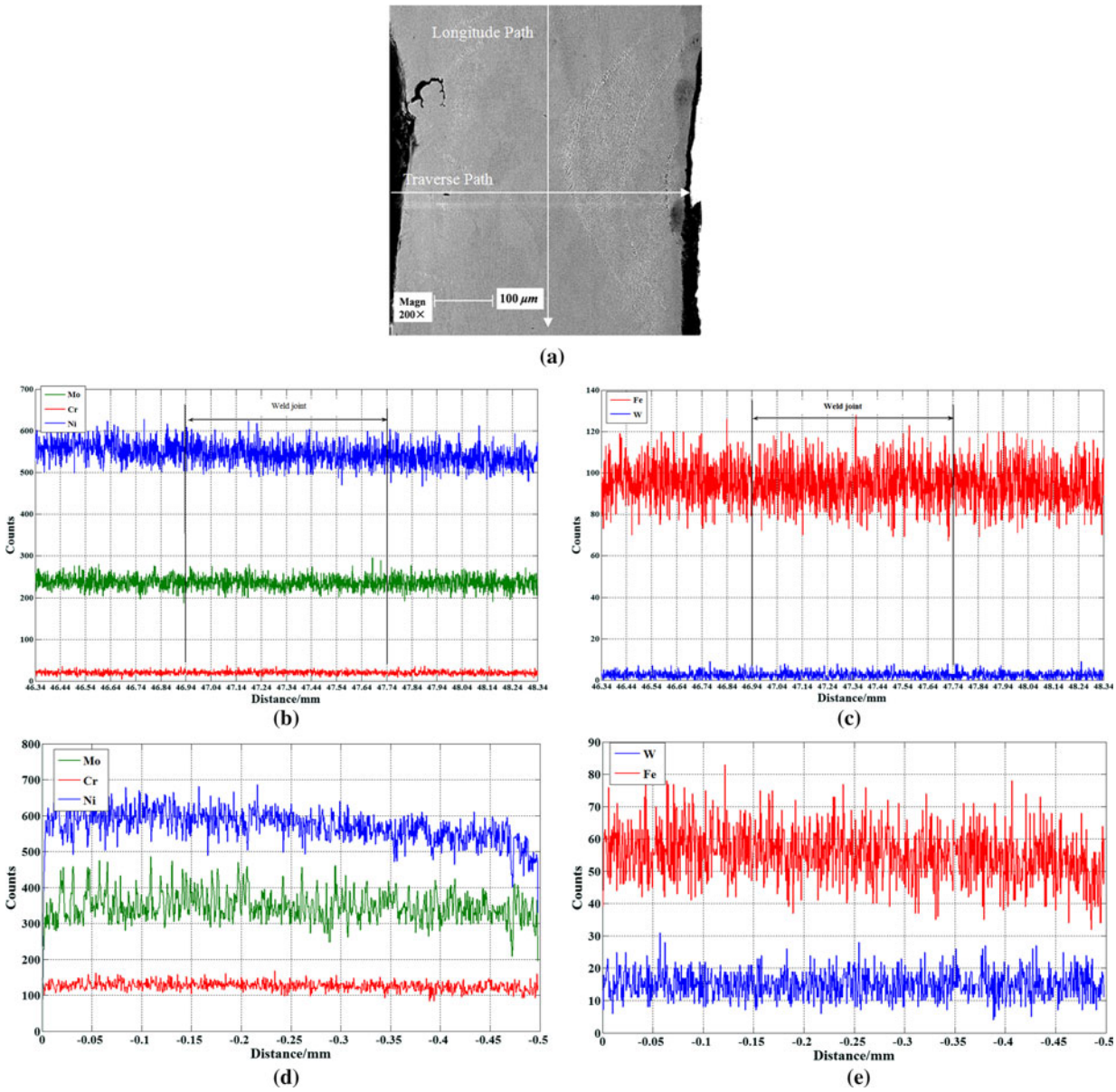

Fig. 4—Macrosegregation testing: (*a*) two scanned paths in the weld joint (welding parameters: 1.5 J, 6 ms, and 30 Hz); (*b*) Ni-Cr-Mo longitude distribution, (*c*) W-Fe longitude distribution, (*d*) Ni-Cr-Mo traverse distribution, and (*e*) W-Fe traverse distribution.

in solid at the solid/liquid interface for $k < 1$ and decrease the concentration of solute for $k > 1$. Thus, the microsegregation of solute at the grain boundary was weakened to some extent.[10,13] In Figure 3(b), the solute distribution calculated by the BF with revised k was given. It was observed, at the large fraction solid, that the trend of elements distribution and composition were more reasonable compared with that calculated by the BF. As a result, during pulsed laser welding, the BF with the revised k could be used to evaluate the solute microsegregation of solid-solution-strengthened Ni-based alloys.

In addition, the macrosegregation is also the important focus during welding.[17] Thus, with the purpose of obtaining in-depth understanding of the macrosegregation behavior during Hastelloy C-276 of pulsed laser welding, the two scanned paths, as shown in Figure 4(a), were selected to evaluate the macrosegregation of the weld joint. In Figures 4(b) through (e), the distributions of the elements Ni, Cr, Mo, Fe, and W in the weld joint were given along the two direction. It was found that the element did not segregate in the weld joint compared with the base metal (shown in Figures 4(b) and (c)), and the element distribution in the wed joint was uniform (shown in Figures 4(d) and (e)). The results indicated that the pulsed laser welding process did not impact the macrodistribution of solute element, and there was no effect of the intermittent action of pulsed laser on the

macrodistribution of the solute element in the weld joint. Consequently, the macrosegregation of the solute element did not occur during the pulsed laser welding.

In summary, by the testing and analysis of microsegregation/macrosegregation of weld joint in pulsed laser welding, it was found the microsegregation was weakened compared with other welding processes, and the Brody-Flemings model with the revised k was proposed to evaluate the element microsegregation of solid-solution-strengthened Ni-based alloys during the pulsed laser welding. Also, no phenomenal macrosegregation was observed in the weld joint as compared with the base metal. The microsegregation/macrosegregation results indicated the process of pulsed laser welding was more suitable to join the Hastelloy C-276 relative to other welding process and could weaken the transformation of brittle phases to some extent.

This research was supported by the National Key Basic Research Program of MOST of P.R. China (Grant No. 2009CB724307) and the National Natural Science Foundation of China (Grant No. 51175061).

REFERENCES

1. J.J. Burton, B.J. Berkowitz, and R.D. Kane: *Metall. Trans. A*, 1979, vol. 10A, pp. 677–82.
2. H.M. Tawancy: *J. Mater. Sci.*, 1981, vol. 16, pp. 2883–89.
3. M.J. Cieslak, G.A. Knorovsky, T.J. Headley, and A.D. Romig, Jr.: *Metall. Trans. A*, 1986, vol. 17A, pp. 2107–16.
4. M.J. Cieslak, T.J. Headley, and A.D. Romig, Jr.: *Metall. Trans. A*, 1986, vol. 17A, pp. 2035–47.
5. J.S. Ogborn, D.L. Olson, and M.J. Cieslak: *Mater. Sci. Eng. A*, 1995, vol. 203, pp. 134–39.
6. M. Ahmad, J.I. Akhter, M. Akhtar, M. Iqbal, E. Ahmed, and M.A. Choudhry: *J. Alloys. Compd.*, 2005, vol. 390, pp. 88–93.
7. F.M. Ghaini, M.J. Hamedi, M.J. Torkamany, and J. Sabbaghzadeh: *Scripta Mater.*, 2007, vol. 56, pp. 955–58.
8. L.M. Liu, H.Y. Wang, and Z.D. Zhang: *Scripta Mater.*, 2007, vol. 56, pp. 473–76.
9. C. Dawes: *Laser Welding*, McGraw-Hill. Inc., UK, 1992, pp. 1–15.
10. J.N. Dupont, J.C. Lippold, and S.D. Kiser: *Welding Metallurgy and Weldability of Nickel - Base Alloys*, John Wiley & Sons, Inc., 2009, pp. 47–150.
11. T.W. Clyne and W. Kurz: *Metall. Trans. A*, 1981, vol. 12A, pp. 965–71.
12. M.J. Aziz: *J. Appl. Phys.*, 1982, vol. 53, pp. 1158–68.
13. W. Kurz and D.J. Fisher: *High Education Press*, Beijing, China, 2010.
14. D.J. Wu, G.Y. Ma, S. Liu, X.Y. Wang, and D.M. Guo: *Appl. Phys. A*, 2010, vol. 101, pp. 517–21.
15. D.J. Wu, G.Y. Ma, Y.Q. Guo, and D.M. Guo: *Phys. Procedia.*, 2010, vol. 5, pp. 99–105.
16. B. Giovanola and W. Kurz: *Metall. Trans. A*, 1990, vol. 21A, pp. 260–63.
17. S. Kou: *Welding Metellurgy*, John Wiley & Sons, Inc., 2002, pp. 145–99.